Fabrication of Architectures with Dual Hollow Structures: Arrays of Cu2O Nanotubes Organized by Hollow Nanospheres

ARTICLE *in* CRYSTAL GROWTH & DESIGN · OCTOBER 2009

Impact Factor: 4.89 · DOI: 10.1021/cg9005339

6 AUTHORS, INCLUDING:

Jun Xu
Hefei University of Technology
38 PUBLICATIONS **1,166** CITATIONS

SEE PROFILE

Weixin Zhang
Hefei University of Technology
105 PUBLICATIONS **2,495** CITATIONS

SEE PROFILE

DOI: 10.1021/cg9005339

CRYSTAL GROWTH & DESIGN Article

2009, Vol. 9
4524–4528

Fabrication of Architectures with Dual Hollow Structures: Arrays of Cu_2O Nanotubes Organized by Hollow Nanospheres

Jun Xu,[†,‡] Yong-Bing Tang,[‡] Weixin Zhang,*[,†] Chun-Sing Lee,*[,‡] Zeheng Yang,[†] and Shuit-Tong Lee[‡]

[†]*School of Chemical Engineering, Hefei University of Technology, Hefei, Anhui 230009, P. R. China,* [‡]*Center of Super-Diamond and Advanced Films (COSDAF) and Department of Physics and Materials Science, City University of Hong Kong, Hong Kong SAR, P. R. China*

Received May 18, 2009; Revised Manuscript Received July 23, 2009

ABSTRACT: Highly ordered array of hierarchical nanotubes constructed from Cu_2O hollow nanospheres with a diameter of 165−185 nm and shell thickness of 20−40 nm has been synthesized by using an array of $Cu(OH)_2$ nanorods as a sacrificial template. The formation of Cu_2O nanotubes is considered to be the result of the "Kirkendall effect", while evolution of the Cu_2O hollow nanospheres from solid nanospheres in the walls results from the "Ostwald ripening" process. Furthermore, the Kirkendall effect in nanoscaled synthesis has been directly proven by the successful design and synthesis of arrays of Cu_2O/$Cu_{2-x}Se$ heterogeneous nanotubes constructed from Cu_2O hollow seminanospheres covered on both the inner and the outer surfaces of $Cu_{2-x}Se$ sheaths with a thickness about 5−10 nm, in which the diffusion rate of copper ions through the $Cu_{2-x}Se$ sheaths is shown to be double that of ascorbic acid molecules during the reaction process. This work offers a new strategy to study the diffusion rate relationship between diffusion couple in nanoscaled synthesis and provides a novel approach for controllable synthesis of hierarchical architectures with dual hollow nanostructures.

1. Introduction

Self-assembly and organization of nanostructured building blocks into complex architectures open up new opportunities for development of materials with designed novel properties and for device fabrication.[1−5] Many recent efforts have been devoted to the controllable organization of primary building blocks into hollow structures, as these hollow structures have various potential applications in drug delivery, chemical sensing, catalysis, artificial cells, lightweight filler, and photonic crystals.[6−12] In most cases, the hollow assemblies were built with solid building blocks. Recently, multiple-walled hollow nanostructures have been prepared through different synthetic strategies. Examples include multiple-shelled Cu_2O nanospheres,[13] multiple-walled Au/Ag alloy nanotubes,[14] and arrays of double-walled copper chalcogenide nanotubes,[15] etc. Different from these multiple-walled hollow structures, hierarchical hollow structures constructed from hollow primary building units have never been reported.

As a p-type semiconductor with a direct band gap of 2.17 eV and unique optical and magnetic properties, Cu_2O is a promising material with applications in solar energy conversion,[16] gas sensing,[17] CO oxidation,[18] lithium ion batteries as electrodes,[19] photocatalytic degradation of organic pollutants,[20,21] and decomposition of water under visible light.[22] Many recent efforts have been devoted to the synthesis of Cu_2O micro- and nanocrystals with various morphologies, such as nanospheres,[17] nanocubes,[20] nanooctahedra,[21] nanopolyhedra,[23,24] nanoplates,[25] nanowires,[26,27] hollow nanospheres,[28] and nonspherical nanocages.[29,30] Nanotube represents an important structural type for nanomaterials. However, there are few reports on the growth of Cu_2O nanotubes,[31] due to its primitive cubic crystal structures. To our best knowledge, there has been no report on the synthesis of vertically aligned arrays of Cu_2O nanotubes. Herein, we report a facile method to prepare highly ordered arrays of Cu_2O nanotubes made of hollow nanospheres based on the "Kirkendall effect" coupled with "Ostwald ripening" by using arrays of $Cu(OH)_2$ nanorods as sacrificial templates. Furthermore, growth of arrays of Cu_2O/$Cu_{2-x}Se$ heterogeneous nanotubes constructed from Cu_2O hollow seminanospheres on both the inner and outer surfaces of thin $Cu_{2-x}Se$ sheaths has also been designed and successfully achieved. This provides direct evidence on the Kirkendall diffusion by mass movement of copper ions and ascorbic acid molecules with different diffusion rates through the $Cu_{2-x}Se$ sheaths.

2. Experimental Section

Synthesis of the Array of $Cu(OH)_2$ Nanorods on Copper Substrate. Synthesis of the $Cu(OH)_2$ nanorod array precursors has been described in detail elsewhere.[32]

Synthesis of the Array of Cu_2O Nanotubes Constructed from Hollow Nanospheres. An array of the $Cu(OH)_2$ nanorods on a copper substrate was immersed in 25−50 mL of ascorbic acid solution (0.005−0.015 M) and kept in a water bath at 55 °C for about 60 min. The product was then carefully taken out of the solution, rinsed sequentially with distilled water and ethanol, and dried in a vacuum.

Synthesis of the Array of Heterogeneous $Cu_2O/Cu_{2-x}Se$ Nanotubes. A Se^{2-} source solution was first prepared by putting 0.005−0.01 g of Se and 0.005−0.015 g of $NaBH_4$ into 50 mL of NaOH solution (0.005 M). A $Cu(OH)_2$ nanorod array on copper foil was immersed in the Se^{2-} solution and kept in it for 2−20 min to prepare the $Cu(OH)_2/Cu_{2-x}Se$ core/sheath nanorod array. The nanorod array was then converted to a nanotube array by immersion in 25−50 mL of ascorbic acid solution (0.005−0.015 M) kept in a water bath at 55 °C for about 60 min. The product was then taken out of the solution, rinsed with distilled water and ethanol, and finally dried in a vacuum.

Characterization of the Samples. The as-prepared samples were characterized by X-ray powder diffraction in a Rigaku D/max-γB

*To whom correspondence should be addressed. E-mail: wxzhang@hfut.edu.cn (W.Z.); apcslee@cityu.edu.hk (C.S.L.).

 Published on Web 08/18/2009

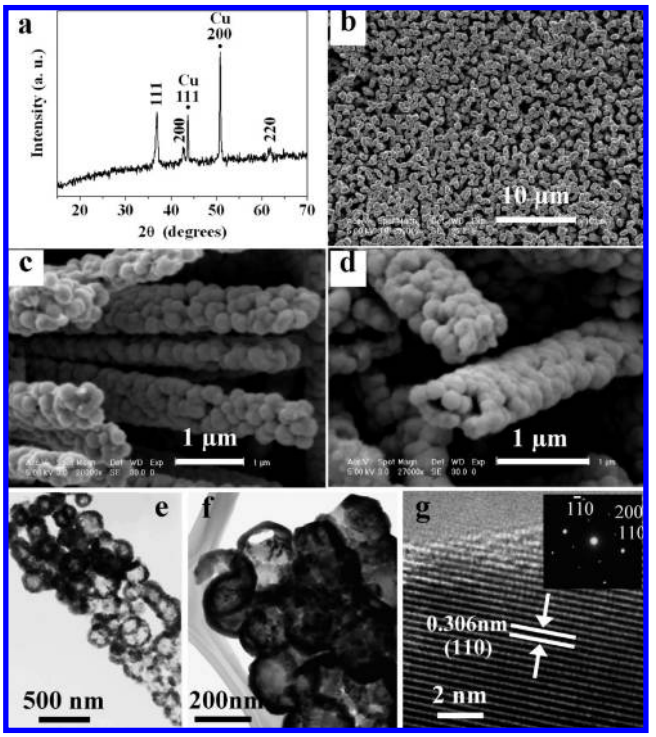

Figure 1. (a) XRD spectrum, (b−d) SEM, and (e,f) TEM images of the Cu_2O nanotubes constructed from hollow nanospheres; (g) high-resolution TEM image of a hollow Cu_2O nanosphere. Inset of (g): SAED pattern of a hollow Cu_2O nanosphere.

or a Rigaku D/max-2400 X-ray diffractometer with a Cu Kα radiation source. Scanning electron microscopy (SEM) was carried out with a JEOL-7500B field-emission scanning electron microscope. Transmission electron microscopic (TEM) images were taken with a Hitachi H-800, a JEOL-2010, or a Philips CM 200 FEG transmission electron microscope operated at 200 kV.

3. Results and Discussion

Figure 1a shows an X-ray diffraction (XRD) spectrum of the product prepared by reducing an array of $Cu(OH)_2$ nanorods on a copper substrate in ascorbic acid solution. Other than the two diffraction peaks (marked with •) from the copper substrate, all the other peaks match well with those of cubic Cu_2O (JCPDF 05-0667). Figure 1b shows a top view of the highly ordered array of Cu_2O one-dimensional (1D) nanostructures which have a similar morphology to that of the $Cu(OH)_2$ nanorod array precursor (Supporting Information, Figure S1). A higher magnification image (Figure 1c) of the Cu_2O nanostructures shows that their sheaths are composed of nanospheres with diameters of 165−185 nm. To determine whether these 1D closed-tip nanostructures have hollow interiors, the Cu_2O array film is slightly scraped to break off the tips. Morphologies of the broken nanostructures (marked with arrows in Figure S2, Supporting Information) show that the 1D nanostructures have hollow interiors. It can be seen from Figure 1d that the walls of the nanotubes are built from one layer of densely packed nanospheres.

A TEM image (Figure 1e) shows that the nanospheres in the nanotube also have hollow interiors. The shell thickness of the hollow nanospheres is estimated to be 20−40 nm from a higher magnification TEM image (Figure 1f). The high-resolution TEM image in Figure 1g of a typical nanosphere shows lattice fringes with a spacing of 0.306 nm which corresponds to the spacing of the (110) planes in Cu_2O.

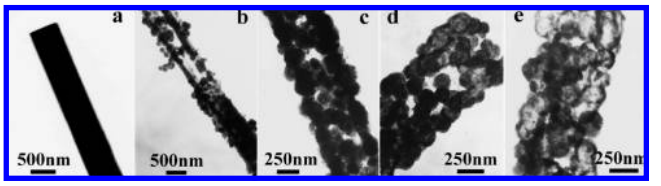

Figure 2. TEM images showing the formation process of the Cu_2O nanotubes. (a) $Cu(OH)_2$ nanorod; (b) $Cu(OH)_2/Cu_2O$ core/sheath nanostructure; (c) Cu_2O nanotube constructed from solid nanospheres; (d) evolution of the Cu_2O solid nanospheres into hollow nanospheres; (e) a nanotube constructed from hollow Cu_2O nanospheres.

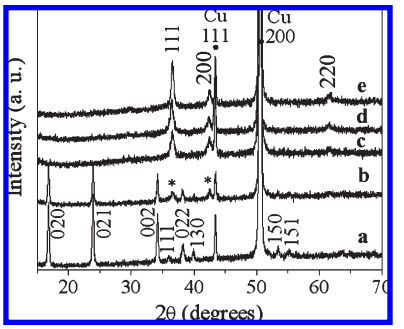

Figure 3. XRD spectra showing the formation process of the Cu_2O nanotubes. (a) $Cu(OH)_2$ nanorods; (b) $Cu(OH)_2/Cu_2O$ core/sheath nanostructures; (c) Cu_2O nanotubes constructed from solid nanospheres; (d) evolution of the Cu_2O solid nanospheres into hollow nanospheres; (e) Cu_2O nanotubes constructed from hollow nanospheres.

The inset SAED pattern of a single hollow nanosphere can be indexed to the [001] zone axis of cubic Cu_2O. The TEM data confirm that the shell of hollow nanospheres is single crystalline. The above results demonstrate that large-scale arrays of hierarchical Cu_2O nanotubes constructed from hollow nanospheres have been successfully fabricated. This unique Cu_2O product shows a multilevel of structures: Cu_2O hollow nanospheres → nanotubes → array of the Cu_2O nanotubes. Because of the unique architecture, this novel array of hierarchical nanotubes might find applications in areas such as delivery systems, storage systems, catalysis, chemical sensing and separation, etc.

To understand the formation mechanism of the hierarchical nanotubes array, we tracked the temporal evolution of the hierarchical nanotube growth. It revealed that the nanotubes were formed by the Kirkendall effect, while the hollow nanospheres were formed through Ostwald ripening. TEM images of the samples at different reaction stages are shown in Figure 2. Figure 2a shows a TEM image of the $Cu(OH)_2$ nanorod precursor, revealing that the nanorod has smooth surfaces and a diameter about 600 nm. Upon immersion in the ascorbic acid solution, $Cu(OH)_2/Cu_2O$ core/sheath nanostructures were first obtained as shown in Figure 2b. After about 30 min of reaction, the $Cu(OH)_2$ core was completely converted to Cu_2O. It should be noted that the Cu_2O nanospheres (Figure 2c) had solid interiors when they were first formed. As time elapsed, the Cu_2O solid nanospheres gradually evolved into hollow nanospheres as shown in Figure 2d. After about 60 min of reaction, hierarchical nanotubes with walls made of Cu_2O hollow nanospheres were formed (Figure 2e). The corresponding XRD spectra of the products at different stages are shown in Figure 3. The diffraction peaks of Cu_2O (spectra c−e) show stronger intensity and narrower

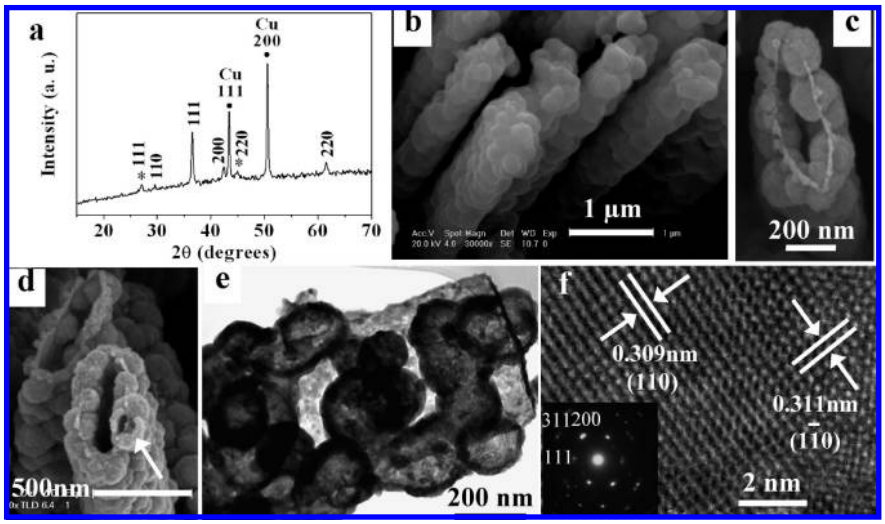

Figure 4. (a) XRD spectrum, (b−d) SEM, and (e) TEM images of the heterogeneous $Cu_2O/Cu_{2-x}Se$ nanotubes constructed from Cu_2O hollow nanospheres and $Cu_{2-x}Se$ sheaths; (f) high-resolution TEM image of a single hollow Cu_2O nanospheres. Inset of (f): SAED pattern of a nanosphere.

width as the reaction time increases, indicating the crystallinity of Cu_2O is improved during the evolution process from solid nanospheres into hollow nanospheres.

The conversion of solid $Cu(OH)_2$ nanorods to hollow Cu_2O nanotubes is believed to be the result of the Kirkendall effect.[33−35] In our process, when the array of $Cu(OH)_2$ nanorods is immersed in the ascorbic acid solution, a thin layer of Cu_2O is first nucleated and formed on the surface of each $Cu(OH)_2$ nanorod. This thin Cu_2O layer acts as an interface that separates the inner copper ions or $Cu(OH)_2$ from the outside ascorbic acid molecules. Thus, direct chemical reaction is hindered, and further reaction depends on outward diffusion of copper ions and/or inward diffusion of ascorbic acid molecules through the interface via vacancy exchanges, in a way similar to the formation of cobalt sulfide hollow nanospheres[33] and hollow polyhedron nanocrystals of Cu_7S_4.[35] At the same time, there will be a concentration gradient of ascorbic acid molecules (Fick's first law) normal to the surface of the $Cu(OH)_2$ nanorods. This will drive the inward diffusion of ascorbic acid through the Cu_2O layer. Copper ions and ascorbic acid molecules react to produce Cu_2O crystallites which aggregate into polycrystalline nanospheres (see the Supporting Information, Figure S3) around the interface. Continuous outward movement of the copper ions will evacuate interiors of the nanorods and further result in the formation of nanotubes.

Further transformation of the polycrystalline Cu_2O solid nanospheres into single-crystal hollow nanospheres in the nanotubes is considered to result from Ostwald ripening.[36,37] The polycrystalline solid nanospheres are assembled from Cu_2O nanoparticles. As shown in Figure 2d, the solid spheres gradually transform to hollow spheres. It is considered that the Cu_2O nanospheres go through a recrystallization process (i.e., Ostwald ripening) and lead to the void formation. Because the smaller crystallites located at central cores have a higher surface energy, they tend to drift to the surface regions during Ostwald ripening. The Cu_2O crystallites on the shell coalesce and become larger ones on attracting the smaller crystallites nearby, and the Cu_2O shells are further crystallized and can eventually become single crystalline through Ostwald ripening.[38,39]

To further study the diffusion rates of the diffusion couple (copper ions and ascorbic acid molecules) in the Kirkendall effect, an array of $Cu_2O/Cu_{2-x}Se$ heterogeneous nanotubes constructed from Cu_2O hollow nanospheres and thin $Cu_{2-x}Se$ sheaths was prepared by reducing an array of $Cu(OH)_2/Cu_{2-x}Se$ core/sheath nanorods in an ascorbic acid solution. Figure 4a shows the XRD spectrum of the heterogeneous products. All the diffraction peaks can be well indexed to cubic Cu_2O (JCPDF 05-0667), except that the two peaks marked with * are due to cubic $Cu_{2-x}Se$ (JCPDF 06-0680) and the two peaks marked with • are due to the copper substrate. Figures 4b shows the array of well-aligned $Cu_2O/Cu_{2-x}Se$ heterogeneous nanotubes with closed-tips and diameters of 500−800 nm. It can be seen that the wall of the nanotubes is also constructed from many nanospheres. Hollow interiors of these nanotubes are demonstrated by cutting off the tips as shown in Figure S4 (Supporting Information). Figure 4c,d shows typical SEM images of some broken $Cu_2O/Cu_{2-x}Se$ nanotubes, revealing that the nanospheres in the tube walls have diameters of 165−185 nm. A broken sphere (marked with an arrow) can also be seen in Figure 4d, which confirms the sphere is hollow. Interestingly, all the Cu_2O hollow nanospheres are actually separated by a thin $Cu_{2-x}Se$ layer into hemispheres. The SEM image in Figure S5 (Supporting Information) shows some broken $Cu_2O/Cu_{2-x}Se$ heterogeneous nanotubes, in which some of the hollow hemispheres are removed from the nanotubes. Chemical composition and morphologies of the $Cu_{2-x}Se$ layer have been confirmed by complete dissolution of the inner $Cu(OH)_2$ cores by immersing the array of $Cu(OH)_2/Cu_{2-x}Se$ core/sheath nanostructures in an ammonia solution as shown in Supporting Information (Figures S6 and S7).

Figure 4e shows a TEM image of the heterogeneous nanotube, revealing that the thickness of $Cu_{2-x}Se$ sheath is 5−10 nm, and the shell thickness of the hollow Cu_2O nanospheres is 20−40 nm. An SAED pattern (inset Figure 4f) of the hollow hemi-nanospheres along the $[01\bar{1}]$ zone axis indicates that the Cu_2O shell is well crystallized, which is corroborated by the high-resolution TEM image in Figure 4f. The fringe of the planes (110) is 0.309 nm and the fringe of the planes $(1\bar{1}0)$ is 0.311 nm. Formation process of the heterogeneous $Cu_2O/Cu_{2-x}Se$ nanotubes is similar to that of homogeneous

Scheme 1. Schematic Illustration of the Formation Processes of Arrays of Hierarchical Cu_2O Nanotubes

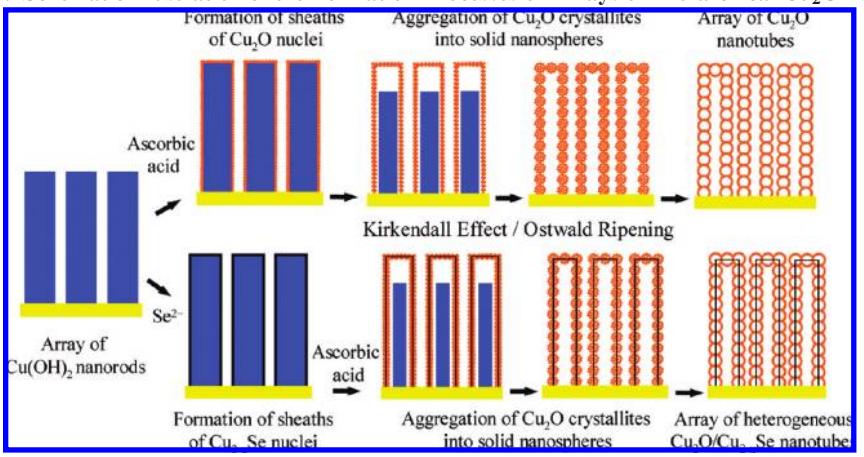

Cu_2O nanotubes as demonstrated by TEM images shown in Figure S8 (Supporting Information). The formations of the two hierarchical nanostructures via the Kirkendall effect and Ostwald ripening are schematically depicted in Scheme 1.

Formation of Cu_2O on the inner and outer surfaces of the $Cu_{2-x}Se$ sheath requires the inward diffusion of ascorbic acid molecules and the outward diffusion of copper ions through the $Cu_{2-x}Se$ sheath, respectively. Therefore, the formation of Cu_2O hollow hemispheres on both the inner and the outer surfaces of the $Cu_{2-x}Se$ sheath confirms that both outward diffusion of copper ions and inward diffusion of ascorbic acid molecules through the thin $Cu_{2-x}Se$ sheath occur during the reaction process. In our case, the redox reaction can be formulated as follows:

$$2Cu(OH)_2+C_6H_8O_6 \rightarrow Cu_2O+C_6H_6O_6+3H_2O$$

On the basis of Figure 4c,d, the volume fractions of Cu_2O on the two sides of the $Cu_{2-x}Se$ sheath are estimated to be about the same, which suggests the molar (mass) fractions of Cu_2O on the two sides of the $Cu_{2-x}Se$ sheath are also about the same, as the mass density of Cu_2O is constant. The diffusion couples have the same diffusion area and diffusion time. Therefore, the diffusion rate (flux density) of copper ions through the $Cu_{2-x}Se$ sheath is roughly twice that of ascorbic acid molecules at the experimental conditions, as the reaction stoichiometric ratio of copper ions and ascorbic acid molecules is 2:1. In fact, the diffusion rates are determined by the reaction temperature. The SEM images of heterogeneous $Cu_2O/Cu_{2-x}Se$ nanotubes obtained at different reaction temperatures are shown in Figure 5, revealing distortion of the heterogeneous nanotubes and dissociation of Cu_2O nanospheres from the $Cu_{2-x}Se$ sheaths at higher temperature. Higher reaction temperature accelerates the diffusion rates. High diffusion rates of copper ions and ascorbic acid molecules through the $Cu_{2-x}Se$ sheaths press the $Cu_{2-x}Se$ nanotubes, and consequently lead to the break and distortion of the heterogeneous $Cu_2O/Cu_{2-x}Se$ nanotubes.

Since the Kirkendall effect was first introduced for the fabrication of hollow nanostructures,[40] it has been widely applied for the synthesis of hollow nanocages within nanoparticles.[7,10,35] Until now, our results give direct experimental evidence on the Kirkendall effect involving simultaneous diffusion of the diffusion couple at different rates. On the other hand, the facile yet controlled formation of high-ordered arrays of hierarchical nanotubes that accentuate the hierarchy, porosity, and anisotropy will facilitate

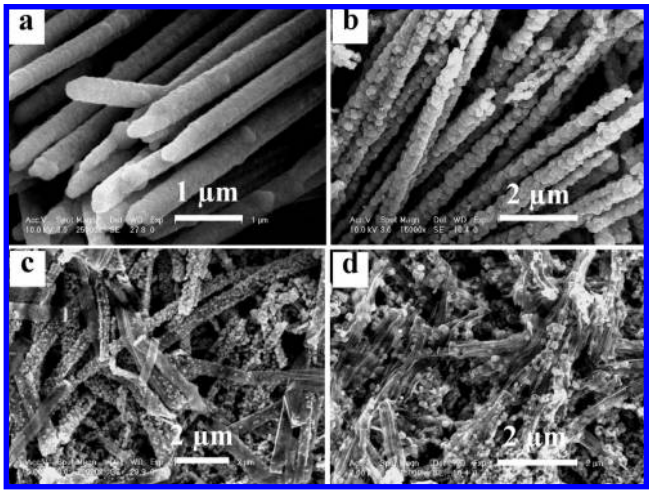

Figure 5. SEM images of the heterogeneous products prepared by using arrays of $Cu(OH)_2/Cu_{2-x}Se$ core/sheath nanorods as precursors at different temperature for 60 min. (a) 25 °C, (b) 40 °C, (c) 70 °C, and (d) 80 °C.

nanostructured materials processing and help to meet design criterions of future devices. We envisage this synthesis strategy can be applied to fabricate many other hollow nanostructures with hierarchy.

4. Conclusions

In summary, highly ordered arrays of hierarchical nanotubes constructed from Cu_2O hollow nanospheres with diameters of 165−185 nm have been synthesized by reducing arrays of $Cu(OH)_2$ nanorods in ascorbic acid. The shell thickness of the hollow Cu_2O nanospheres is in the range of 20−40 nm. Formation of the nanotubes is attributed to the Kirkendall effect, while evolution of single-crystalline Cu_2O hollow nanospheres from polycrystalline solid nanospheres is considered to result from Ostwald ripening. The synthesis of the $Cu_2O/Cu_{2-x}Se$ heterogeneous nanotubes with hierarchy has also been demonstrated by using arrays of $Cu(OH)_2/Cu_{2-x}Se$ core/sheath nanorods as precursors. The wall of these heterogeneous nanotubes is constructed from Cu_2O hollow nanospheres with diameters of 165−185 nm separated by thin $Cu_{2-x}Se$ layers with a thickness of 5−10 nm, resulting in formation of unique hemihollow nanospheres on both the inner and outer sides of $Cu_{2-x}Se$ tubes. The formation of

$Cu_2O/Cu_{2-x}Se$ heterogeneous nanotubes provides direct evidence on the Kirkendall effect in nanotube synthesis, in which the diffusion rates of copper ions through the $Cu_{2-x}Se$ sheaths is estimated to be nearly double that of ascorbic acid molecules.

Acknowledgment. This work was financially supported by the City University's Research Enhancement Scheme, the National Natural Science Foundation of China (NSFC Grants 20871038, 20876031), the Education Department of Anhui Provincial government (TD200702) and the Research Grants Council of HKSAR, CRF grant no. CityU5/CRF/08.

Supporting Information Available: SEM images of the $Cu(OH)_2$ nanorod array; SEM images of some broken Cu_2O nanotubes and broken heterogeneous $Cu_2O/Cu_{2-x}Se$ nanotubes; XRD spectra, TEM and SEM images of the sheath-like $Cu_{2-x}Se$ nanotubes; TEM images for the evolution process of the heterogeneous $Cu_2O/Cu_{2-x}Se$ nanotubes. This information is available free of charge via the Internet at http://pubs.acs.org.

References

(1) Caruso, F.; Caruso, R. A.; Mohwald, H. *Science* **1998**, *282*, 1111.
(2) Whitesides, G. M.; Grzybowski, B. *Science* **2002**, *295*, 2418.
(3) Dinsmore, A. D.; Hsu, M. F.; Nikolaides, M. G.; Marquez, M.; Bausch, A. R.; Weitz, D. A. *Science* **2002**, *298*, 1006.
(4) Liu, B.; Yu, S. H.; Li, L. J.; Zhang, Q.; Zhang, F.; Jiang, K. *Angew. Chem., Int. Ed.* **2004**, *43*, 4745.
(5) Tian, Z. R.; Liu, J.; Voigt, J. A.; Mckenzie, B.; Xu, H. *Angew. Chem., Int. Ed.* **2003**, *42*, 413.
(6) Yuan, J.; Laubernds, K.; Zhang, Q.; Suib, S. L. *J. Am. Chem. Soc.* **2003**, *125*, 4966.
(7) Yang, J. H.; Qi, L. M.; Lu, C. H.; Ma, J. M.; Cheng, H. M. *Angew. Chem., Int. Ed.* **2005**, *44*, 598.
(8) Bigi, A.; Boanini, E.; Walsh, D.; Mann, S. *Angew. Chem., Int. Ed.* **2002**, *41*, 2163.
(9) Liu, B.; Zeng, H. C. *J. Am. Chem. Soc.* **2004**, *126*, 8124.
(10) Liu, B.; Zeng, H. C. *J. Am. Chem. Soc.* **2004**, *126*, 16744.
(11) Caruso, F. *Chem.—Eur. J.* **2000**, *6*, 413.
(12) Zhang, W. X.; Luan, C. Y.; Yang, Z. H.; Liu, X. T.; Zhang, D. P.; Yang, S. H. *Appl. Surf. Sci.* **2007**, *253*, 6063.
(13) Xu, H. L.; Wang, W. Z. *Angew. Chem., Int. Ed.* **2007**, *46*, 1489.
(14) Sun, Y. G.; Xia, Y. N. *Adv. Mater.* **2004**, *16*, 264.
(15) Xu, J.; Zhang, W. X.; Yang, Z. H.; Yang, S. H. *Inorg. Chem.* **2008**, *47*, 699.
(16) Briskman, R. N. *Sol. Energy Mater. Sol. Cells* **1992**, *27*, 361.
(17) Zhang, J. T.; Liu, J. F.; Peng, Q.; Wang, X.; Li, Y. D. *Chem. Mater.* **2006**, *18*, 867.
(18) White, B.; Yin, M.; Hall, A.; Le, D.; Stolbov, S.; Rahman, T.; Turro, N.; O'Brien, S. *Nano Lett.* **2006**, *6*, 2095.
(19) Poizot, P.; Laruelle, S.; Grugeon, S.; Dupont, L.; Taracon, J. M. *Nature* **2000**, *407*, 496.
(20) Kuo, C. H.; Chen, C. H.; Huang, M. H. *Adv. Funct. Mater.* **2007**, *17*, 3773.
(21) Xu, H. L.; Wang, W. Z.; Zhu, W. *J. Phys. Chem. B* **2006**, *110*, 13829.
(22) Hara, M.; Kondo, T.; Komoda, M.; Ikeda, S.; Shinohara, K.; Tanaka, A.; Kondo, J. N.; Domen, K. *Chem. Commun.* **1998**, 357.
(23) Siegfried, M. J.; Choi, K. S. *J. Am. Chem. Soc.* **2006**, *128*, 10356.
(24) Siegfried, M. J.; Choi, K. S. *Angew. Chem., Int. Ed.* **2005**, *44*, 3218.
(25) Ng, C. H. B.; Fan, W. Y. *J. Phys. Chem. B* **2006**, *110*, 20801.
(26) Tan, Y. W.; Xue, X. Y.; Peng, Q.; Zhao, H.; Wang, T. H.; Li, Y. D. *Nano Lett.* **2007**, *7*, 3723.
(27) Wang, W. Z.; Wang, G. H.; Wang, X. S.; Zhan, Y. J.; Liu, Y. K.; Zheng, C. L. *Adv. Mater.* **2002**, *14*, 67.
(28) Chang, Y.; Teo, J. J.; Zeng, H. C. *Langmuir* **2005**, *21*, 1074.
(29) Teo, J. J.; Chang, Y.; Zeng, H. C. *Langmuir* **2006**, *22*, 7369.
(30) Kuo, C. H.; Huang, M. H. *J. Am. Chem. Soc.* **2008**, *130*, 12815.
(31) Cao, M. H.; Hu, C. W.; Wang, Y. H.; Guo, Y. H.; Guo, C. X.; Wang, E. B. *Chem. Commun.* **2003**, 1884.
(32) Zhang, W. X.; Xu, J.; Yang, Z. H.; Ding, S. X. *Chem. Phys. Lett.* **2007**, *434*, 256.
(33) Yin, Y. D.; Rioux, R. M.; Erdonmez, C. K.; Hughes, S.; Somorjai, G. A.; Alivisatos, A. P. *Science* **2004**, *304*, 711.
(34) Wang, Y. L.; Cai, L.; Xia, Y. N. *Adv. Mater.* **2005**, *17*, 473.
(35) Cao, H. L.; Qian, X. F.; Wang, C.; Ma, X. D.; Yin, J.; Zhu, Z. K. *J. Am. Chem. Soc.* **2005**, *127*, 16024.
(36) Liu, B.; Zeng, H. C. *Small* **2005**, *1*, 566.
(37) Yang, H. G.; Zeng, H. C. *J. Phys. Chem. B* **2004**, *108*, 3492.
(38) Zhu, L. P.; Xiao, H. M.; Zhang, W. D.; Yang, G.; Fu, S. Y. *Cryst. Growth Des.* **2008**, *8*, 957.
(39) Xu, H. L.; Wang, W. Z.; Zhou, L. *Cryst. Growth Des.* **2008**, *8*, 3486.
(40) Sun, Y. G.; Xia, Y. N. *Science* **2002**, *298*, 2176.